

Surface-roughness contributions to the electrical resistivity of polycrystalline metal films

U. Jacob, J. Vancea, and H. Hoffmann

Institut für Angewandte Physik, Universität Regensburg, D-8400 Regensburg, Germany

(Received 1 December 1989)

The influence of surface roughness on the electrical conductivity of polycrystalline metal films has to be considered at two different length scales. The large-scale surface roughness due to the granular arrangement of these films gives rise to a fluctuating film cross section. One-dimensional models of these fluctuations lead to roughness values consistent with scanning-tunneling-microscopy images of film surfaces. The microscopic surface roughness, mainly given by atomic steps on the crystallite surfaces, represents centers for surface scattering of conduction electrons. With this concept we were able to describe not only the thickness-dependent conductivity of films with natural (as-deposited) surface roughness, but also the increase in the resistance during subsequent coating with adatoms at 80 K owing to an artificial microscopic roughening of their surfaces.

I. THE PROBLEM

The electrical resistivity of thin metal films is increased by surface scattering, as soon as the mean free path (MFP) of the conduction electrons (CE) is comparable to the film thickness. Distortions in the smooth surface potential give rise to diffuse surface scattering and therefore to an enhanced resistivity (size effect). The surface roughness of evaporated polycrystalline films consequently gives an important contribution to their resistivity.

Figure 1 shows a scanning-tunneling-microscopy (STM) image taken from the surface of a 30-nm-thick polycrystalline copper film with a mean crystallite size of $D=24$ nm; the film was evaporated at 2×10^{-10} mbar on a Corning glass substrate held at 300 K. Height fluctuations typically of 4–6 nm with 50–60 nm lateral extension are the major features of this surface topology. The CE's cannot surely be scattered at these hillocks, because the roughness scale is much larger than their Fermi wavelength ($\lambda_F \approx 0.5$ nm). Therefore, the influence of the roughness at large scale (e.g., MFP scale) should be treated in a different way than that of atomic scale (e.g., λ_F

scale). This was first proposed by Namba,¹ applied quantitatively by Vancea and co-workers,^{2–5} and recently discussed by Trivedi and Ashcroft.⁶

According to Fig. 1 the cross section of a polycrystalline metal film is roughly suggested in Fig. 2. The large-scale surface roughness H gives rise to thickness fluctuations, whereas the roughness at atomic scale (h) is responsible for the potential involved to the surface scattering of CE's. Consequently, the mean conductivity $\langle \sigma(d) \rangle$ at a mean thickness d can be calculated by the following:^{1,2,6}

$$\langle \sigma(d) \rangle = \frac{L}{d} \left[\int_0^L dx \frac{1}{\sigma(d(x))d(x)} \right]^{-1} \quad (1)$$

with L the length of the film and $d(x)=f(H(x))$ the thickness fluctuation along the current path. The function $\sigma(d(x))=f(\sigma_\infty, l_\infty, d(x), g(h))$ describes the conductivity at the local thickness $d(x)$, i.e., a reduced value compared with the corresponding infinitely thick film

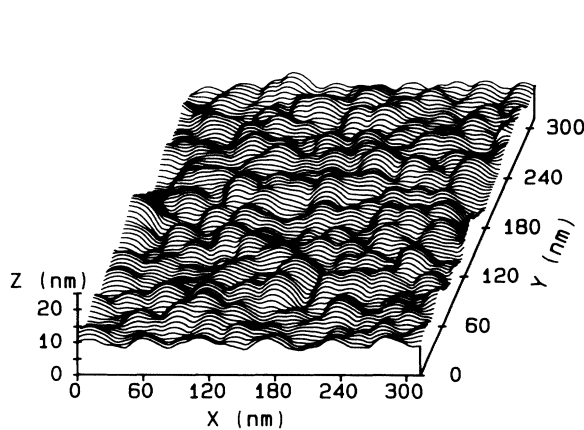


FIG. 1. Scanning-tunneling-microscopy surface topography of an evaporated (2×10^{-10} -mbar 300 K) polycrystalline copper film.

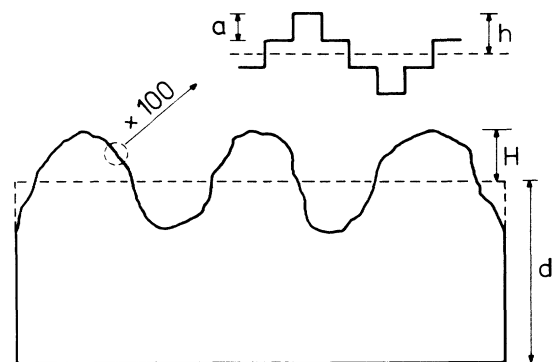


FIG. 2. Rough drawing of the cross section of polycrystalline metal films. H denotes surface roughness at mesoscopic scale, h the surface roughness at microscopic scale, d the mean film thickness, and a the atomic steps of height a .

(σ_∞, l_∞). The surface scattering is given by the scattering function $g(h)$.

A. The scattering of CE's at microscopic surface irregularities

1. The classical model of Fuchs (Ref. 7)

In this model the function $g(h)$ is described by a phenomenological specularity parameter (p), i.e., by the probability for specular reflection of CE's at the surface. Indeed there is no direct connection with the scattering mechanism itself. The thickness-dependent conductivity is given by

$$\frac{\sigma(d(x))}{\sigma_\infty} = 1 - \frac{3(1-p)}{2k} \times \int_1^\infty dt \left[\frac{1}{t^3} - \frac{1}{t^5} \right] \frac{1 - \exp(-kt)}{1 - p \exp(-kt)}, \quad (2)$$

where σ_∞ denotes the conductivity limited only by volume scattering (defects, grain boundaries, etc.), k the $d(x)/l_\infty$, l_∞ the MFP of the CE, p the specularity parameter, and $d(x)$ the local film thickness.

This model was often used to describe the thickness-dependent conductivity. The fitting of Eq. (1) [with (2)] to the experimental data gives values of the parameters σ_∞ , l_∞ , p , and H . The value of specularity (p) can be correlated with the surface potential at microscopic scale. For platinum films, for instance, the specularity p is proportional to the relative contribution of the (111) orientation to the total surface area,⁸ i.e., to that part of the surface which does not undergo surface reconstruction. Consequently, the specularity depends on the roughness at microscopic (atomic) scale.

2. The classical "surface roughness model" of Soffer (Ref. 9)

Comparable to the scattering of light on rough surfaces (Kirchhoff formalism) the specularity p depends on the angle of incidence (θ) of the CE's and on the ratio h/λ_F .^{9,10} For uncorrelated surface roughness it follows that

$$p(\cos(\theta)) = \exp \left[- \left[\frac{4\pi h}{\lambda_F} \right]^2 \cos^2 \theta \right]. \quad (3)$$

Equation (3) allows nonzero specularity only for $h/\lambda_F \ll 1$. The model of Soffer was extensively applied by Sambles and co-workers¹¹ to the thickness-dependent conductivity of polycrystalline gold films. They obtained values of $h < 0.05$ nm, i.e., a tenth of atomic distances. These results are indeed unrealistic.

3. The quantum-mechanical surface-roughness model of Tešanović, Jaric, and Maekawa (Ref. 12)

In this model the microscopic variations of the surface profile are related to a set of pseudopotentials acting on

the quantum states of a system with the same average thickness but smooth surfaces. The Hamiltonian of the system is given by

$$\chi = \chi_{\parallel} + \chi_{d(x,y)}(z), \quad (4)$$

where χ_{\parallel} describes extended states in the parallel space and $\chi_{d(x,y)}(z)$ denotes the variable length scale of the confining potential.

For uncorrelated surface roughness the thickness dependence of σ treated within the Kubo formalism is described by

$$\frac{\sigma(d(x))}{\sigma_\infty} = \frac{1}{n_c} \sum_{n=1}^{n_c} \left[1 + \frac{l_\infty}{l_{\max}} n^2 \right]^{-1} \quad \text{for } n_c \gg 1, \quad (5)$$

where $n_c = k_F d(x)/\pi$, the number of subbands in the k space located at the Fermi level, and $l_{\max} = 6\pi n_c^2 d(x)/(k_F^2 \hbar^2)$.

In contrast to the semiclassical model of Soffer a finite conductivity results for $l_\infty \rightarrow \infty$ ($T=0$) instead of $\sigma \rightarrow \infty$ (classical case). This model has been successfully applied to the treatment of the electrical conductivity in very-thin epitaxial CoSi₂ films ($d = 1$ nm).¹³

A similar formalism has been also used recently by Trivedi and Ashcroft⁶ for the treatment of the conductivity in size quantized Pt films.

B. Large-scale surface irregularities

In order to describe the influence of the surface roughness at large scale, the film will be divided into segments of length l_∞ and mean thickness d . An electron traveling from one segment to another loses phase coherence. Therefore, the propagation at this length scale can be described semiclassically, i.e., by Eq. (1). This problem was first treated by Namba¹ and recently discussed by Trivedi and Ashcroft.⁶ Namba used the Fuchs formula (2) for $\sigma(d(x))$ in Eq. (1) with

$$d(x) = d + H \sin(2\pi x/s) \quad (6)$$

and H and s as the large-scale roughness and roughness wavelength, respectively.

Trivedi and Ashcroft⁶ used instead of Eq. (6) a Gaussian distribution with a mean thickness d and rms deviation H . In a quantum-mechanical formalism for $\sigma(d(x))$ they were able to describe the results of Hoffmann and co-workers¹⁴ for Pt films with $H = 0.5$ nm.

It should be noted, however, that equally good results with similar values of H have been obtained by Vancea and co-workers^{2,3,5} for the same Pt films within the Fuchs-Namba formalism. Instead of Eq. (6) we additionally tried (in some cases) a Gaussian-distributed thickness fluctuation.^{2,3} For the Cu films considered in Fig. 1 we obtained for three fitting parameters ($\sigma_\infty, l_\infty, p$) similar values in both cases, i.e., within the accuracy of the assessment procedure (see Ref. 5). Solely the surface roughness H showed larger values exceeding by about 20% those obtained with Eq. (6). This discrepancy, however, cannot be significant (see also Fig. 1) resulting only from the different approximations of the thickness fluctuation. Additionally, the fits with a Gaussian surface

profile were of slightly poorer quality as those involving Eq. (6).

The Namba formalism is quite simple and restricts the number of fitting parameters to four. Within this formalism we were able to describe the thickness-dependent conductivity of a large number of polycrystalline metals. The main requirement concerning the validity of the Namba formalism is as follows:

$$H/L_c \ll 1,$$

where L_c is the roughness correlation length. The STM image of Fig. 1 indeed shows $H/L_c \leq 0.1$, and therefore the use of Eq. (1) with $d(x)$ given by Eq. (6) seems to be justified.

The intention of this paper is to discuss the surface scattering of CE's at microscopic surface irregularities from an experimental point of view. In a first step we compare the results of the three models discussed above fitted to the thickness-dependent conductivity of films with natural (as-deposited) surface roughness. Due to the reasons discussed above we use Eq. (1) here with $d(x)$ given by Eq. (6). Subsequent coating of these films with proper adatoms increases the surface scattering of CE's because of their artificial roughening at microscopic scale. In a second step, therefore, we discuss the behavior of the electrical conductivity during metal-metal adsorption in view of the models of surface scattering at microscopic surface roughness.

II. RESULTS AND DISCUSSION

A. Copper films of natural surface roughness (as-deposited on Corning glass)

Figure 3 shows the thickness-dependent conductivity of copper films ($D = 24$ nm) deposited in UHV (2×10^{-10} mbar) on Corning glass held at 300 K. The experimental procedure was described in Ref. 2. The fitted curves

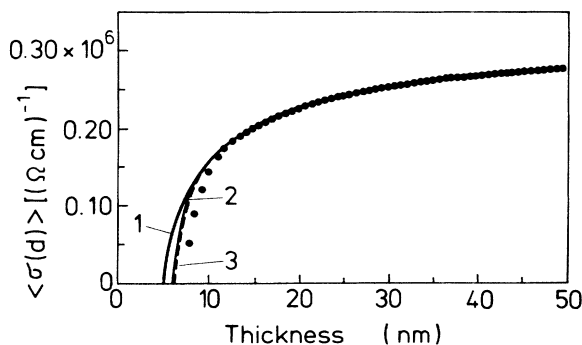


FIG. 3. Thickness-dependent conductivity of copper films prepared in 2×10^{-10} mbar on Corning glass held at 300 K. The dotted lines represent measured values, whereas the solid line denotes fitted models of (1) Fuchs-Namba [$\sigma_\infty = 0.32 \times 10^6$ ($\Omega \text{ cm})^{-1}$, $l_\infty = 26$ nm, $p = 0.42$, and $H = 5$ nm], (2) Soffer-Namba [$\sigma_\infty = 0.32 \times 10^6$ ($\Omega \text{ cm})^{-1}$, $l_\infty = 23$ nm, $h = 0.096$ nm, and $H = 6.2$ nm], and (3) Tešanović-Namba [$\sigma_\infty = 0.33 \times 10^6$ ($\Omega \text{ cm})^{-1}$, $l_\infty = 26$ nm, $h = 0.33$ nm, and $H = 6$ nm].

(solid lines) correspond to the models of surface scattering described above; these have been introduced in Eq. (1) in order to comprise the additional effect of large-scale fluctuations. Whereas for the Fuchs-Namba and Soffer-Namba model a full four-parameter fit could be applied, a value of $l_\infty = 26$ nm was embraced in the Tešanović-Namba model. Since only linear terms in l_∞ and h are present in Eq. (5), it is impossible to separate these parameters by computer fitting.

All three models give comparable results concerning σ_∞ , l_∞ , and H . The large-scale surface roughness H is comparable to the value resulting from the STM image of Fig. 1. Concerning the surface scattering of CE's, only the Fuchs-Namba and the Tešanović-Namba models give physical results, i.e., the following:

(i) The model of Soffer gives unrealistic values of the microscopic surface roughness ($h = 0.07$ – 0.1 nm for about 20 films).

(ii) On the contrary, h amounts to 0.28–0.33 nm in the model of Tešanović (for about 20 films); consequently, h is comparable to atomic steps (terraces) on crystallite surfaces.

(iii) In the model of Fuchs we find $p = 0.42$ (e.g., $0 \leq p \leq 1$).

The following discussion will be restricted to the model of Tešanović, which gives a realistic description of the surface scattering of CE's at microscopic surface roughness.

B. Artificially roughened thin-film surfaces

Coating with adatoms gives rise to an enhanced surface scattering. The dominant scattering mechanism depends on the nature of these adatoms: If the atoms of the base layer and the adatoms have different valences, the Coulomb scattering is predominant.¹⁵ If both materials have the same number of electrons per atom, the surface potential will be altered only due to a variation of the microscopic surface roughness in the first stage of coating. The change in the resistance with increasing thickness of the coating layer, therefore, will depend on the growth mechanism during metal-metal adsorption.

1. Model of metal-metal adsorption

The growth mechanism during the metal-metal adsorption was simulated by a computer algorithm in a similar way as Chauvineau¹⁶ and Schumacher.¹⁷ The surface of a crystallite is represented by a 100×100 matrix. Since the next-neighbor distance of the copper atoms is 0.24 nm, this procedure reflects realistic conditions on polycrystalline copper surfaces with a mean crystallite size of 24 nm. Before coating, an ideal flat surface has been assumed. Each atom of the surface is surrounded by eight neighbors. Anisotropic surface diffusion has been excluded. Only isolated atoms can move on the surface, i.e., clusters formed by at least two atoms will be already stable. Condensation and diffusion events on the surface are simulated by random numbers. The influence of the adatom's mobility is given by the mobility parameter w as follows:

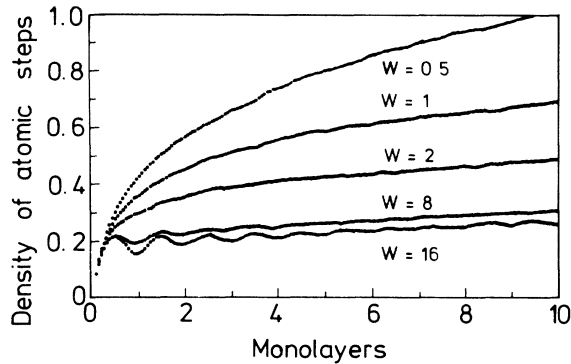


FIG. 4. Computer simulation where the increase of density of atomic steps during coating is plotted as a function of surface mobility w .

$$w = \frac{\nu \exp[-Q/(kT)]}{(dn/dt)A}, \quad (7)$$

where ν denotes the surface phonon frequency, Q the activation energy for surface jumps, dn/dt the condensation rate, and A the surface unit.

The surface roughness is characterized by the density of atomic steps on the crystallite surface caused by the condensed adatoms as follows:

$$h = 0.5as, \quad (8)$$

where a denotes the next-neighbor distance for copper ($a = 0.24$ nm) and s the density of atomic steps. This value was calculated from the actual number of created atomic steps (of height a) divided by the total number of available adsorption sites, i.e., 10^4 in our model.

For uncorrelated surface profiles, the value of H calculated from Eq. (8) corresponds fairly well with the rms value of the surface roughness.

Figure 4 shows the role of the mobility parameter w for the subsequent roughening of the presumed ideal flat surfaces. The microscopic surface roughness will be reciprocal to the mobility of the adatoms, i.e., reciprocal to the condensation temperature and proportional to the condensation rate. If the surface mobility is adequately high, even periodic changes of the microscopic roughness can be expected, leading to nearly flat surfaces at full coverage (layer-by-layer growth). With aid of the mobility parameter w both islandlike or layer-by-layer growth can be simulated within the adsorption model presented.

2. Copper adatoms on copper base layers

The experiments were performed in 2×10^{-10} mbar without breaking the vacuum between the evaporation of base and coating layers. Experimental details are given in Ref. 18.

Figure 5 shows the change in the resistance during coating of copper base layers (prepared at 300 K) with copper adatoms. If the adatoms are condensed at 300 K the resistance decreases immediately with the adsorption of few copper atoms; for condensation at 80 K, however, the resistance passes through a maximum. This behavior

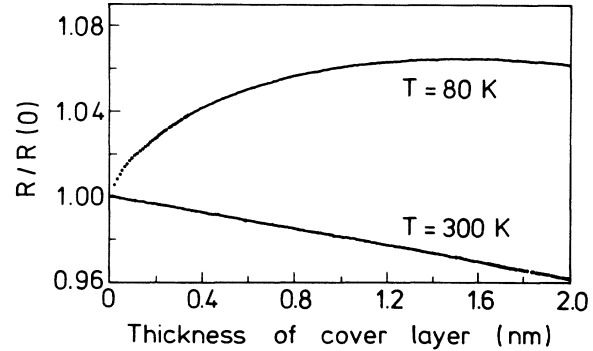


FIG. 5. Change in the resistance of a copper film prepared at 300 K during coating with copper adatoms at 300 and 80 K.

can only be explained by an artificial roughening of the base-layer surface during the metal absorption at 80 K. The mobility of the adatoms at 300 K is sufficiently enough to reach steps and stacking faults on the surface. In contrast to this, the mobility at 80 K strongly decreases. Consequently, the adatoms are adsorbed at flat surface regions, and the surface roughness increases. This results in an enhancement of the resistance due to the increased surface scattering. If the surface scattering becomes completely diffuse, we observe a saturation followed by a decrease in the resistance due to the increased thickness of the double layer.

Figure 6 shows the relative change in the resistance for 30-nm-thick copper films versus the added thickness during adatom's coating at 80 K and various evaporation rates. As shown the relative change in the resistance during metal-metal adsorption depends very sensitively on the evaporation rate, i.e., on the adatom's surface mobility. Consequently, we can try to explain the experimental results of Fig. 6 with the adsorption model previously presented. The change in the resistance was calculated within the Tešanović-Namba formalism where the values of the microscopic surface roughness resulted from the density of the created atomic steps. For these calcula-

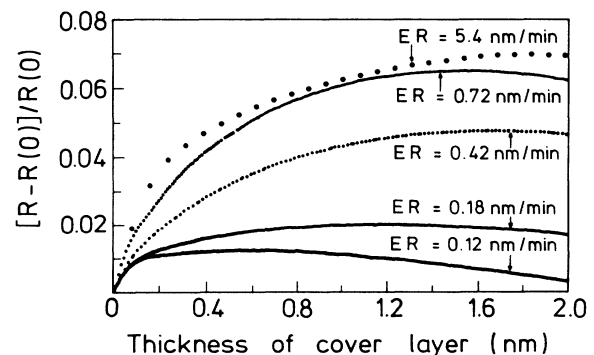


FIG. 6. Relative change of the resistance during coating of Cu films with Cu adatoms at 80 K and different evaporation rates (ER). Thickness of the base layer is 30 nm.

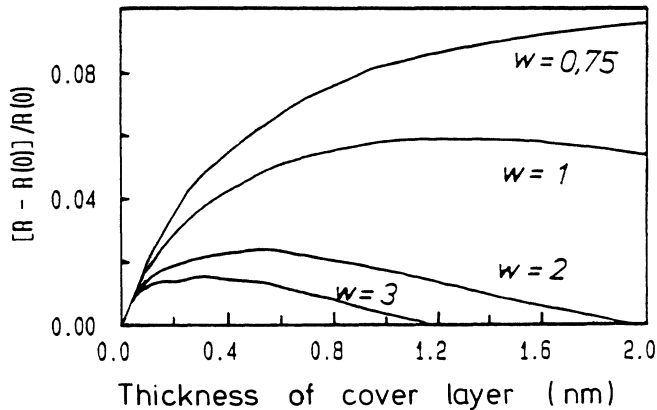


FIG. 7. Influence of surface mobility on the relative change of the resistance: computer simulation with the model of Tešanović-Namba.

tions we used $l_{\infty}(80 \text{ K}) = 60 \text{ nm}$ resulting from the application of Matthiessen's rule to l_{∞} :

$$\frac{1}{l_{\infty}(80 \text{ K})} = \frac{1}{l_{\infty}(300 \text{ K})} - 21.8 \times 10^{-3} \text{ nm}^{-1} \quad (9)$$

with $l_{\infty}(300 \text{ K}) = 26 \text{ nm}$. The free term in Eq. (9) results from the values of the electron-phonon scattering lengths at 300 and 80 K, respectively. Such values can be calculated, for instance, from data given in Ref. 19. The results of the computer simulations are given in Fig. 7. Both, the qualitative behavior and order of magnitude for the relative increase in the resistance can be well described by the absorption model previously discussed. The values of the parameter w used in the computer simulating can be directly correlated to the different condensation rates. One notices, for example, that an increase of w by a factor of four gives the same increase in resistivity as observed in Fig. 6 by a decrease of the evaporation rate with the same factor. From the fitted values of w and a mean value of $\nu \approx 5 \times 10^{12} \text{ Hz}$,²⁰ the activation energy for surface diffusion of copper atoms on polycrystalline copper films can be calculated from Eq. (7) to

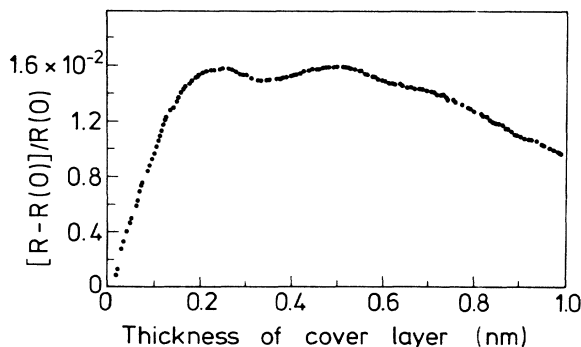


FIG. 8. Relative change in the resistance of an Al film during coating with Al adatoms at 80 K. Thickness of the base layer is 27 nm.

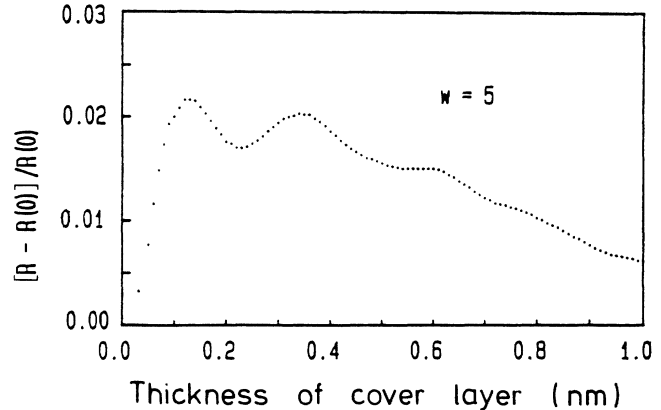


FIG. 9. Results of the computer simulation for Al adsorption on Al: $l_{\infty}(80 \text{ K}) = 50 \text{ nm}$.

$$Q = 0.22 \text{ eV} ,$$

i.e., a value corresponding to the energy of the impinging adatoms.²¹ At low temperatures, therefore, the adatoms seem to move only in the range of one interatomic distance.

3. Aluminum adatoms on aluminum base layers

Figure 8 shows the observed change in the resistance for a 27-nm-thick aluminum film prepared at 300 K and 2×10^{-10} mbar during coating at 80 K with aluminum adatoms. The evaporation rate of the coating layer was 1.56 nm/min.

In addition to the monotonic change in the resistance due to the artificial surface roughening, several oscillations can be observed. The period of these oscillations amounts to $0.25 \pm 0.02 \text{ nm}$, i.e., $(1.5 \pm 0.2) \times 10^{15}$ atoms/cm². An aluminum monolayer contains $(1.2 \pm 0.3) \times 10^{15}$ atoms/cm², if the same mean value for the (111), (110), and (100) directions is considered. The comparison of the values above suggests layer-by-layer growth in this case. The experimental results of Fig. 8 can be well reproduced with aid of the adsorption model previously discussed combined with the Tešanović-Namba formalism. The result of these calculations for a mobility parameter of $w = 5$ is shown in Fig. 9. The value of the MFP in this case amounts to 50 nm, as calculated from the Matthiessen's rule [Eq. (9)] with $l_{\infty}(300 \text{ K}) = 14 \text{ nm}$, (resulted from the Fuchs-Namba fitting²) and a free term of $51.7 \times 10^{-3} \text{ nm}^{-1}$.¹⁹ As is the case of copper adsorbed on copper, the qualitative behavior and order of magnitude for the increase in the resistance can be well described within this formalism. The slightly enhanced mobility of Al on Al compared to Cu on Cu leads to layer-by-layer growth and consequently to oscillations in the electrical resistance.

III. CONCLUDING REMARKS

Surface roughness of polycrystalline metal films gives rise to an increase in their resistivity. The scale of this

roughness, however, has to be considered in order to correctly describe the mechanism leading to the enhanced resistivity.

Two length scales have been considered.

(i) A mesoscopic scale roughness (at the scale of MFP) which mainly produces a fluctuating film cross section. Therefore, a mean conductivity at a mean film thickness value was calculated from the local conductivities affected by surface scattering. This approach requires a model of the thickness fluctuation, which is, in fact, a nontrivial task. Simplified one-dimensional models, however, give a reasonable description of the mean resistivity leading to model-related roughness comparable to values resulting from scanning-tunneling microscopy images of film's surface. This result confirms our earlier analysis of the thickness-dependent conductivity for polycrystalline metal films^{2,3,5} and the recent discussion of Trivedi and Ashcroft.⁶ One notices, however, that the roughnesses discussed in this paper are larger by a factor of 10 than those discussed in Ref. 6. The local conductivities required for the calculation of the mean values can be obtained by a proper consideration of the surface scattering mechanism involved.

(ii) The surface roughness at microscopic scale (e.g., the scale of the Fermi wavelength) is responsible for the diffuse surface scattering of CE's in clean metal films. We comparatively analyzed the thickness-dependent conductivity of polycrystalline copper films with natural (as-deposited) microscopic surface roughness using three different models of surface scattering (e.g., Fuchs,⁷ Soffer,⁹ and Tešanović and co-workers¹²). Although all these models introduced in the averaging formalism of Namba¹ fitted equally well to the experiment, only two of them lead to reasonable results.

(a) The classical model of Fuchs⁷ allowed an independent evaluation of the MFP and specularity by computer fitting; unfortunately the phenomenological description

of the surface scattering in this case offers no direct information about the scattering mechanism itself.

(b) The quantum-mechanical model of Tešanović, Jaric, and Maekawa¹² allowed a direct access to the values of microscopic surface roughness supplying realistic values comparable to atomic steps on crystallite surfaces; unfortunately the separation of the MFP and microscopic surface roughness is not practicable so that the MFP has to be inserted. Through a simultaneous application of the two models previously discussed, however, an *a priori* assumption of the MFP value has been avoided.

Coating experiments at low temperatures giving rise to an artificial microscopic roughening of the "as deposited" film surfaces have been additionally undertaken in order to prove the concept presented above. The increase of the resistance during metal-metal adsorption at low temperatures has been well reproduced with the model of Tešanović and co-workers¹² combined with the formalism of Namba.¹ The value of the MFP necessary for these calculations was determined by fitting of the Fuchs-Namba model to the thickness-dependent conductivity of the uncovered films. Both islandlike and layer-by-layer growth of adatoms on the film surface held at 80 K have been well reproduced with the approach described above.

In summary, we were able to quantitatively describe the influence of the surface roughness on the electrical resistivity of polycrystalline metal films within the following concept.

(i) The large scale surface roughness was treated in a different way than the microscopic one according to our earlier work (Fuchs-Namba formalism) and the recent discussion of Trivedi and Ashcroft.⁶

(ii) The MFP of CE's was determined from the Fuchs-Namba fitting to the thickness-dependent conductivity.

(iii) This MFP was inserted in the Tešanović-Namba formalism in order to describe the surface scattering of CE's at microscopic surface roughness.

¹Y. Namba, *Jpn. J. Appl. Phys.* **9**, 1326 (1970).

²J. Vancea, Ph.D. dissertation, University of Regensburg, 1982; J. Vancea, H. Hoffmann, and K. Kastner, *Thin Solid Films* **121**, 201 (1984); J. Vancea, G. Reiss, and H. Hoffmann, *J. Mater. Sci. Lett.* **6**, 985 (1987).

³H. Hoffmann, in *Festkörperprobleme*, Vol. 22 of *Advances in Solid-State Physics*, edited by J. Treusch (Vieweg, Braunschweig, 1982), p. 255; J. Vancea, *Int. J. Mod. Phys. B* **3**, 1455 (1989).

⁴J. Vancea, G. Reiss, and H. Hoffmann, *Phys. Rev. B* **35**, 6435 (1987).

⁵H. Hoffmann and J. Vancea, *Thin Solid Films* **85**, 147 (1981).

⁶N. Trivedi and N. W. Ashcroft, *Phys. Rev. B* **38**, 12 298 (1988).

⁷K. Fuchs, *Proc. Cambridge Philos. Soc.* **34**, 100 (1938).

⁸H. Hoffmann, J. Vancea, and U. Jacob, *Thin Solid Films* **129**, 181 (1985).

⁹S. B. Soffer, *J. Appl. Phys.* **38**, 1710 (1967).

¹⁰J. M. Ziman, *Electrons and Phonons* (Oxford University Press, London, 1960), p. 456.

¹¹J. R. Sambles, *Thin Solid Films* **106**, 321 (1983).

¹²Z. Tešanović, M. V. Jaric, and S. Maekawa, *Phys. Rev. Lett.* **57**, 2760 (1986).

¹³J. M. Phillips, J. L. Batstone, J. C. Hensel, and M. Cerullo, *Appl. Phys. Lett.* **51**, 1895 (1987).

¹⁴H. Hoffmann, and G. Fischer, *Thin Solid Films* **32**, 25 (1976).

¹⁵R. F. Greene, *Phys. Rev.* **141**, 687 (1966).

¹⁶J. P. Chauvineau and C. Pariset, *J. Cryst. Growth* **53**, 505 (1981).

¹⁷D. Schumacher, Ph.D. dissertation, University of Düsseldorf, 1983.

¹⁸U. Jacob, J. Vancea, and H. Hoffmann, *J. Phys. Condens. Matter* **1**, 9867 (1989).

¹⁹N. W. Ashcroft and N. D. Mermin, *Solid State Physics* (Holt-Saunders, Philadelphia, 1976), Vol. 38, pp. 8–10.

²⁰J. E. Black and F. C. Shanes, *Surf. Sci.* **133**, 199 (1983).

²¹R. V. Stuart, *Vacuum Technology, Thin Films and Sputtering* (Academic, New York, 1983), p. 119.